Downloaded 10/14/21 to 68.97.118.233. Redistribution subject to SEG license or copyright; see Terms of Use at http://library.seg.org/page/policies/terms
DOI:10.1190/segam2021-3594319.1

Applications of Pre-Stack Seismic Inversion on a Silurian Pinnacle Reef Gas Storage Reservoir for Enhanced Geologic Interpretations

Clayton Silver[1], Dr. Heather Bedle[1], Dr. Matthew Rine[2], [1]University of Oklahoma, [2]Consumers Energy*

Summary

Carbonate reservoirs provide numerous complications for accurate reservoir characterization and management. A seismic survey acquired in the Fall of 2019 over a Silurian (Niagaran) pinnacle reef gas storage reservoir is utilized for amplitude variation with offset (AVO) inversion to assist in reservoir characterization to enhance gas storage efficiency. P-impedance and P-wave velocity volumes provide a good delineation of the underlying, non-reservoir facies, and cross-plotting the two inversion attribute volumes allows for classification of on-lapping salt and carbonate seismic facies. Lambda-mu-rho (LMR) analysis allows for identification of porous zones to target for gas storage.

Introduction

The Michigan Basin was a prolific hydrocarbon producer throughout the mid to late 20th century. Niagaran (mid-Silurian) pinnacle reefs were widely produced throughout the basin during this time. Following production, many of these reefs were converted to storage reservoirs for natural gas and carbon sequestration. Despite the widespread production, few stratigraphic models of the internal structure and facies distribution of the reefs has been completed. Rine et al. (2017) provides a core and log-constrained facies model for Niagaran reefs along the southern trend in the Michigan Basin and illustrates that the reefs are composed of distinct, predictable lithofacies. Carbonate reservoirs, especially those that have undergone dolomitization, are characterized by a high degree of vertical and lateral heterogeneity (Pranter et al., 2005). Well data provides excellent vertical constraint on the distribution of reservoir properties; however, provide little spatial constraint. To better understand the spatial distribution of quality reservoir facies, a recently acquired three-dimensional (3-D) seismic survey over Ray Reef, a reef in the southern reef trend, is integrated with tightly-spaced core data.

Field Description

Geologic Setting

The Michigan Basin is an intracratonic basin that exhibits unusual circular symmetry and is bounded by a continuous structurally stable area, and covers an area of 316,000 km^2. The Silurian reefs occur in the upper Niagaran Guelph Formation, also known as the Brown Niagaran, which rims the circular Michigan Basin. The reefs are presently buried at depths of 900 to 2000 m. Individual reefs have average widths of approximately 1000 m and average heights of 100 m. Reef development was concentrated in two parallel lineaments on the northern and southern margins of the basin.

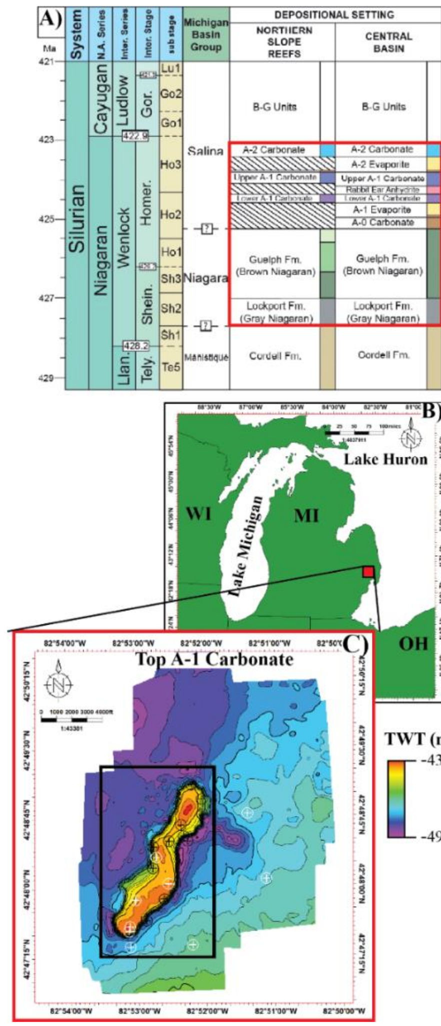

Figure 1: A- Chronostratigraphic chart for the Michigan Basin (After Rine et al., 2017). B- Overview map of the study area. C- TWT structure map of the A1 Carbonate displaying the structure and well locations of the Ray Reef study area. Grey symbols represent cored wells, and white symbols represent wells with sonic or density logs. The black box represents the cropped volume extents used in this study.

The lithostratigraphy of the reefs is well established (Figure 1a). Silurian reefs overly the Lockport Formation (informally called the “Gray Niagaran”), which is a micritic carbonate mudstone. Reefs are laterally encased by the thin limestones and evaporites of the Silurian Salina Group. Reefs along the southern reef trend have undergone

© 2021 Society of Exploration Geophysicists

10.1190/segam2021-3594319.1

extensive dolomotization. Haynie (2009) provides a well-based geostatistical model of petrofacies in Ray Reef, and defined favorable petrofacies as those with greater than 5% porosity and permeability greater than 1mD. Overlying facies within the Upper A1 Carbonate and the upper portion of the reef core were proposed as the highest quality reservoir facies.

<u>Data Description</u>

Petrophysical Dataset

A total of 81 wells are present within the study area. Of these, 20 are cored and have whole-core derived porosity and permeability logs. 11 of the 20 wells have lithofacies descriptions provided by an expert geologist from Consumers Energy. Seven wells have sonic logs and six have density logs (Figure 1c). The remaining wells provide GR, resistivity and neutron logs.

Seismic Dataset

In this study, a 3-D survey with an area of approximately 10 mi^2 acquired in 2019 was used to analyze the internal structure of a Niagaran reef along the southern reef trend (Figure 1c). Both a pre-stack time migrated (PSTM) full-angle stack volume and pre-stack conditioned gathers are available. The survey has a 1 millisecond (ms) sample rate and 2000 ms record length, and a line spacing of 55 ft for both inlines and crosslines. The pre-stack offset gathers were processed by professional geoscientists at Sterling Seismic, and underwent a standard workflow for AVO analyses. The pre-stack gathers are of good quality, and using a smooth velocity model created from sonic logs within the reef reveals that angles up to 30 degrees are present within our interval of interest. The survey was cropped to the limits of the reef for efficient computation of inversion volumes (Figure 1c). Vertical resolution within the reef interval is approximately 45 ft. At the time of acquisition, Ray Reef was at near full storage capacity, as it had 64.5 bcfg out of a total storage capacity of 65.4 bcfg.

Methods

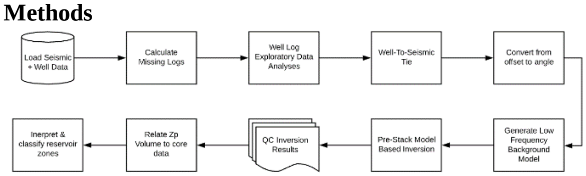

Figure 2: Generalized workflow applied in this study.

<u>Well Log Estimation</u>

Figure 2 provides an overview for the workflow followed in this study. Gardner's relationship between velocity and density is applied to predict the respective missing logs in wells with either sonic or density logs present. Following density and sonic log estimation, shear logs were estimated using the workflow proposed by Xu et al. (2007) which proposes a model whereby limestones contain a variety of pore types which can be modeled by different aspect ratio inclusions. As the reservoir is completely dolomitized, mineralogical estimates for dolomite density were used rather than limestone. A density of 2.87 g/cm^3 were used for dolomite within the reservoir with an aspect ratio of 0.20 for the macroporosity and 0.05 for the microporosity. The calculated Vp/Vs logs do not provide any values below the theoretical limit of 1.41, so the estimated logs are deemed satisfactory given the available data.

<u>Petrophysical Exploratory Data Analyses</u>

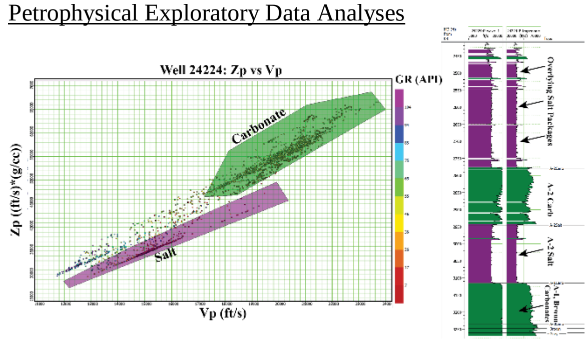

Figure 3: Cross plot of computed P-impedance and measured P-wave velocity. The user-defined polygons correspond to the classified well log shown on the right.

As data limitations prevented accurate petrophysical modeling, the measured well log data were investigated to reveal relationships between measured properties and the geology. The starting point in this study was Well 24224, as it is the only well with both sonic and density logs. P-impedance (Zp) and P-velocity (Vp) are cross-plotted as it

Downloaded 10/14/21 to 68.97.118.233. Redistribution subject to SEG license or copyright; see Terms of Use at http://library.seg.org/page/policies/terms
DOI:10.1190/segam2021-3594319.1

© 2021 Society of Exploration Geophysicists

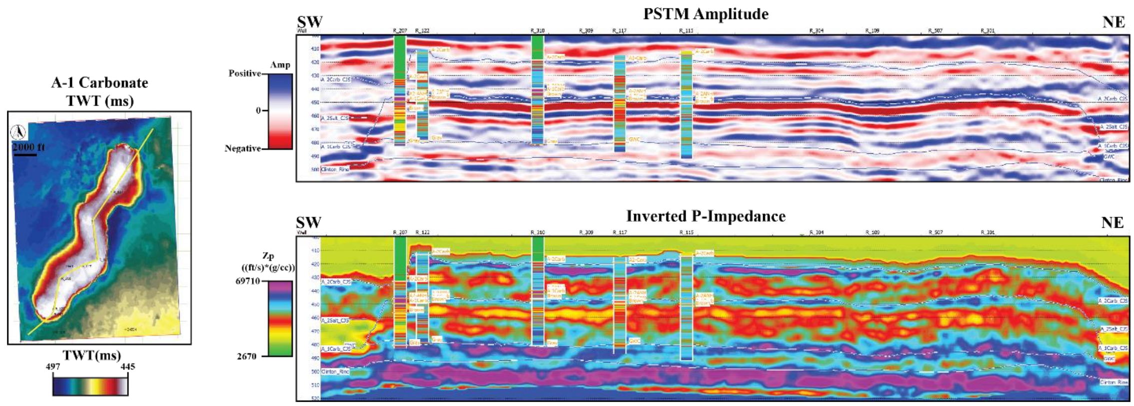

Figure 4: Left- Overview map displaying the arbitrary line location shown to the right. Top – PSTM seismic amplitude with computed Zp logs overlain. Bottom- Inverted Zp cross section with computed Zp logs overlain.

was observed that the A-2 Salt (150 ft thick) has low Zp and Vp values (Figure 3). Defining polygons around these low values indicate that this is an excellent method of classifying the A-2 Salt. Additionally, a polygon created around the data points corresponding to a high Vp and Zp correlate very well to the encountered A-2 Carbonate, A-1 Carbonate, and Brown formation. This suggests that the resulting Zp and Vp volumes produced from inversion can be applied to classify non-reservoir (A-2 Salt) and reservoir (A-1 Carbonate, Brown Fm) away from well locations.

AVO Simultaneous Pre-Stack Inversion

All AVO studies are based on the plane wave Zoeppritzs equations, which model a plane wave in terms of P and S wave velocity and density. However, due to the complexities of Zoeppritzs equations, approximations are commonly used. Pre-stack simultaneous inversion implemented by the Hampson-Russell software utilizes the Fatti et al. (1994) extension of the Aki-Richards (1980) approximation of Zoeppritzs equations (Hampson and Russell, 2005). Fatti et al. reformulated the Aki-Richards formula so that the reflectivity as a function of angle is represented by the P-impedance and S-impedance rather than velocity and density. Integrating the reflectivity component in Fatti's equation provides the P-wave impedance, Zp. The simultaneous inversion method used is a deterministic method – which means the inversion result will provide one single solution that minimizes the error between the initial model and the input seismic data. The goal of the pre-stack inversion is to remove the wavelet from the seismic data and to transition from an interface property (seismic amplitude) to a layer property (impedance) which allows for more direct geologic interpretations (Maurya and Sarkar, 2016).

The low frequency model (LFM) constructed in this study utilized 3 wells: Well 24224, located off the reef, wells R-117, and R-207 which are both located within the reef. Well 24224 was selected as it provides good control of lithologies located off the reef. Well R-117 has a measured sonic log and estimated density log, while well R-207 has a measured density log and estimated sonic log. Additionally, well R-207 provides accurate density values for the capping A-2 Anhydrite. Four interpreted horizons were used as input: The A-2 Carbonate, A-2 Salt, A-1 Carbonate, and the Clinton

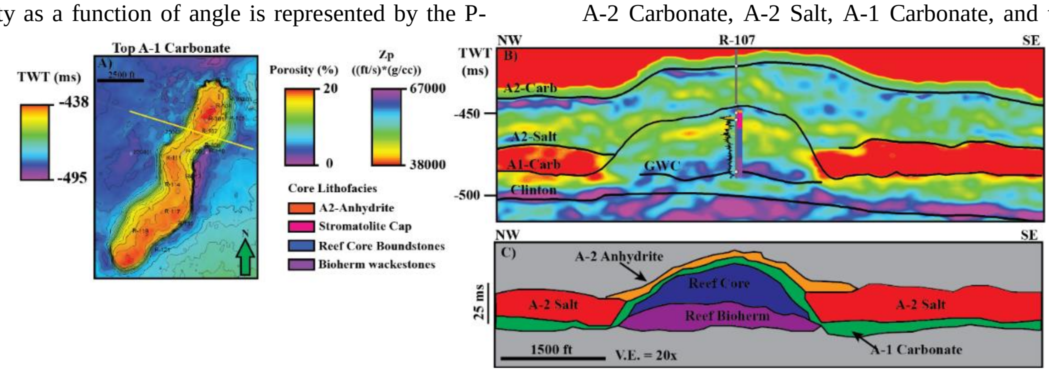

Figure 5: A- overview map displaying the top of the A-1 Carbonate in TWT. The location of B and C is shown by the yellow line. B- Arbitrary line through the Zp volume displaying well R-107 core measured porosity and lithofacies log. C- Geologic interpretation of the vertical seismic display shown in B. Note the inverse relationship between Zp and core measured porosity.

Downloaded 10/14/21 to 68.97.118.233. Redistribution subject to SEG license or copyright; see Terms of Use at http://library.seg.org/page/policies/terms
DOI:10.1190/segam2021-3594319.1

Downloaded 10/14/21 to 68.97.118.233. Redistribution subject to SEG license or copyright; see Terms of Use at http://library.seg.org/page/policies/terms
DOI:10.1190/segam2021-3594319.1

formation horizons. The model honors the stratigraphic relationships of the reef.

Results

Inversion Results

Figure 4 provides a comparison between the PSTM amplitude data and the Zp volume from the pre-stack inversion (Figure 4b,c). A good correlation is observed between the Zp volume and the computed Zp logs in all wells except for R-115. This can be attributed to an erroneous calculated density log from the measured sonic log. Ray Reef is characterized by planar internal reflectors which decrease in strength toward the base of the reef and become more discontinuous. Uncertainties arise when trying to interpret the extent of the reef core and bioherm and little geologic information can be extracted from the seismic amplitude directly. In the seismic amplitude, it is also difficult to differentiate the overlying A-1 Carbonate from the A-2 Anhydrite (Figure 4b). Well log data indicates that these units are just below the estimated resolution of the seismic data but should be detectable. The A-2 Anhydrite ranges in thickness to 30 to 50 feet and the A-1 Carbonate ranges from 30 to 45 feet thick above Ray Reef. By removing the effect of the wavelet and analyzing the Zp transect, the two units can now be distinguished, as the A-2 Anhydrite is characterized by high Zp values due to its high density and Vp values (Figure 4c). At well R-107 this becomes apparent, as overlaying the core lithology data on the Zp data allows for correlation between Zp values and core lithofacies (Figure 5b,c). The A-2 Anhydrite correlates with the thin high Zp layer overlying the reef. Additionally, the low porosity, heavily cemented reef bioherm facies correspond to a region of high Zp values near the base of the reef. The reef core is characterized by mid to high porosity and lower Zp values. Prior to the seismic inversion, mapping of the low-porosity reef bioherm was not possible from the PSTM amplitude.

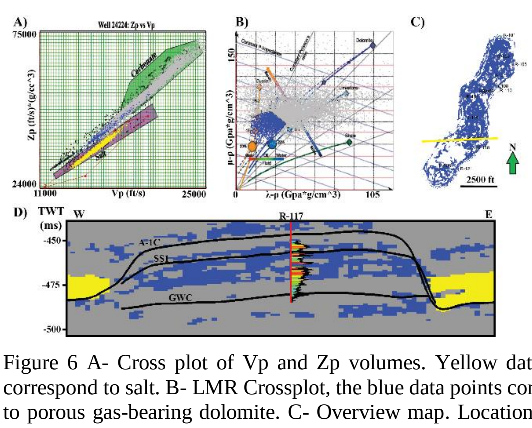

Figure 6 A- Cross plot of Vp and Zp volumes. Yellow data points correspond to salt. B- LMR Crossplot, the blue data points correspond to porous gas-bearing dolomite. C- Overview map. Location of D is shown in yellow. The classified volume is extracted along stratal slice 1 to show the spatial distribution of porous facies. D- Transect through the classified seismic volume using the cross plots shown in A and B. The core-measured porosity log at well R-117 is overlain.

Seismic Facies Classification

Using the relationship shown in Figure 3 between Zp and Vp, the two equivalent inversion volumes were cross-plotted to classify the onlapping A-2 Salt. Using the Sound-QI software QI-Pro, the well log cross plot from Figure 3 is applied as a guide to classifying the seismic facies. While the values in the inversion data are slightly higher for both Vp and Zp, the same trend is observed. The A-2 Salt is captured very well by the same trends observed in well log data. Using the Zp and Zs inversion attributes, lambda-rho and mu-rho (LMR) volumes were calculated (Russell, 2003). The blue seismic facies was classified using a data-driven approach by following the template of Goodway et al., 1997.

Investigation boxes were drawn around zones of high-porosity observed from core data. Points within these investigation boxes were then highlighted in cross-section and classified by a polygon. The classified zones correlate well with core data, and delineates porous gas-bearing dolomite within the reservoir. The good lateral distribution of reservoir rock with vertical discontinuities correlates with previous well-based reservoir models (Haynie, 2009). It is important to note that porous zones are predicted within the overlying A-2 Carbonate, which are likely erroneous and suggests further refinement is needed for this classification.

Conclusions

A pre-stack simultaneous inversion was carried out over a mid-Silurian pinnacle reef in the eastern Michigan Basin. Due to the limited well log data set available, no reliable shear volumes were produced. Analyses of the Vp and Zp volumes integrated with available core data allows for detailed geologic interpretations of the reef complex. The Zp inversion attribute allow for discrimination of the A-2 Anhydrite from the A-1 Carbonate. Using in-context geologic knowledge combined with well data observations allows for interpretation of the non-reservoir reef bioherm facies between well locations. These interpretations allow for more accurate mapping of key lithological units compared to interpretations made on seismic amplitude data. Relationships observed in well log data between Zp and Vp were directly translated to seismic data to classify the laterally encasing A-2 Salt and gas-bearing carbonate lithologies. An attempt to classify porous facies was made with good success within the reservoir, but over-predicted porous facies outside of the pinnacle reef reservoir.

Acknowledgments

We would like to thank Consumer’s Energy for providing the seismic and well data used for this study. We would also like to thank CGG and Schlumberger for donating software licenses used for enhanced visualization and interpretation. Finally, we thank AASPI for funding this study.

© 2021 Society of Exploration Geophysicists

10.1190/segam2021-3594319.1

REFERENCES

Aki, K., and P. G. Richards, 1980, Quantitative seismology: W.H. Freeman & Co.

Fatti, J. L., G. C. Smith, P. J. Vail, P. J. Strauss, and P. R. Levitt, 1994, Detection of gas in sandstone reservoirs using AVO analysis: A 3D seismic case history using the Geostack technique: Geophysics, **59**, 1362–1376, doi: https://doi.org/10.1190/1.1443695.

Goodway, B., T. Chen, and J. Downton, 1997, Improved AVO fluid detection and lithology discrimination using Lamé petrophysical parameters;"λρ","μρ", & "λ/μ fluid stack", from P and S inversions: SEG Technical Program, Expanded Abstracts, 183–186, doi: https://doi.org/10.1190/1.1885795.

Hampson, D. P., B. H. Russell, and B. Bankhead, 2005, Simultaneous inversion of pre stack seismic data: SEG Technical Program, Expanded Abstracts, doi: https://doi.org/10.1190/1.2148008.

Haynie, J. M., 2009, Characterization and modeling of petrofacies and pore volume distribution within a gas storage reservoir, Ray Reef Field, Southern Michigan Basin, Michigan: Thesis directed by Associate Professor Matthew J. Pranter, M.S. Geology, Department of Geological Sciences.

Maurya, S. P., and P. Sarkar, 2016, Comparison of post stack seismic inversion methods : A case study from Blackfoot Field, Canada: International Journal of Scientific and Engineering Research, **7**, 1091–1101.

Pranter, M. J., C. B. Hirstius, and D. A. Budd, 2005, Scales of lateral petrophysical heterogeneity in dolomite lithofacies as determined from outcrop analogs: Implications for 3-D reservoir modeling: AAPG Bulletin, **89**, 645–662, doi: https://doi.org/10.1306/11300404049.

Rine, M. J., J. D. Garrett, and S. E. Kaczmarek, 2017, A new facies architecture model for The Silurian Niagaran Pinnacle Reef Complexes of the Michigan Basin: Characterization and Modeling of Carbonates–Mountjoy Symposium 1.

Russell, B. H., K. Hedlin, F. J. Hilterman, and L. R. Lines, 2003, Fluid property discrimination with AVO: A Biot Gassmann perspective: Geophysics, **68**, 29–39, doi: https://doi.org/10.1190/1.1543192.

Xu, S., G. Chen, Y. Zhu, J. Zhang, M. Payne, M. Deffenbaugh, and J. H. Dunsmuir, 2007, Carbonate rock physics: Analytical models and validations using computational approaches and lab/log measurements: International Petroleum Technology Conference.

Downloaded 10/14/21 to 68.97.118.233. Redistribution subject to SEG license or copyright; see Terms of Use at http://library.seg.org/page/policies/terms
DOI:10.1190/segam2021-3594319.1